β Phorbol Ester- and Diacylglycerol-Induced Augmentation of Transmitter Release Is Mediated by Munc13s and Not by PKCs

Jeong-Seop Rhee,[1,7] Andrea Betz,[2,7,8]
Sonja Pyott,[1,7] Kerstin Reim,[2,3]
Frederique Varoqueaux,[2,3] Iris Augustin,[2,3]
Dörte Hesse,[3] Thomas C. Südhof,[4]
Masami Takahashi,[5] Christian Rosenmund,[1,6]
and Nils Brose[2,3,6]
[1] Abteilung Membranbiophysik
Max-Planck-Institut für Biophysikalische Chemie
Am Faßberg 11
D-37077 Göttingen
Bundesrepublik Deutschland
[2] Abteilung Molekulare Neurobiologie
[3] Abteilung Neurogenetik
Max-Planck-Institut für Experimentelle Medizin
Hermann-Rein-Straße 3
D-37075 Göttingen
Bundesrepublik Deutschland
[4] Howard Hughes Medical Institute
University of Texas Southwestern Medical Center
Center for Basic Neuroscience
Department of Molecular Genetics
6000 Harry Hines Boulevard
Dallas, Texas 75390
[5] Mitsubishi Kasei Institute of Life Sciences
Machida, Tokyo 194-8511
Japan

Summary

Munc13-1 is a presynaptic protein with an essential role in synaptic vesicle priming. It contains a diacylglycerol (DAG)/β phorbol ester binding C_1 domain and is a potential target of the DAG second messenger pathway that may act in parallel with PKCs. Using genetically modified mice that express a DAG/β phorbol ester binding-deficient Munc13-1^{H567K} variant instead of the wild-type protein, we determined the relative contribution of PKCs and Munc13-1 to DAG/β phorbol ester-dependent regulation of neurotransmitter release. We show that Munc13s are the main presynaptic DAG/β phorbol ester receptors in hippocampal neurons. Modulation of Munc13-1 activity by second messengers via the DAG/β phorbol ester binding C_1 domain is essential for use-dependent alterations of synaptic efficacy and survival.

Introduction

Changes in the efficacy of synaptic transmission between neurons mediate adaptive properties of the brain and contribute to learning and memory processes. Alterations of synaptic strength, which are best characterized in synaptic long-term potentiation, occur in diverse brain regions and involve successive, spatially segregated modulations of pre- and postsynaptic processes (Malenka and Nicoll, 1999). Presynaptically, changes in the shape of action potentials, the size and duration of Ca^{2+} transients, or the refilling kinetics and size of readily releasable vesicle pools (RRPs) can contribute to transient and long-term increases in evoked synaptic transmitter release (Hawkins et al., 1993; Nayak and Browning, 1999).

Apart from physiological stimuli such as high-frequency action potential trains, increases in presynaptic efficacy in many neurons are readily induced by β phorbol esters (β-PEs; Majewski and Iannazzo, 1998). These functional analogs of the endogenous second messenger diacylglycerol (DAG) bind with high affinity to the zinc finger-like C_1 domains of a diverse group of mammalian DAG/β-PE receptor proteins, including PKCs α, βI, βII, γ, δ, ε, η, θ, μ, and ν, Munc13-1, -2, and -3, α1/2 and β1/2 chimaerins, and RasGRP (Kazanietz et al., 2000). The mechanism by which DAG and β-PEs regulate presynaptic function is important because modulation of transmitter release by G protein-coupled receptors via increased DAG production represents a regulatory second messenger pathway that controls synaptic transmission. Numerous pharmacological experiments indicate that β-PEs (and thus DAG) enhance transmitter release by activating PKCs. Indeed, the strong stimulation of presynaptic function by β-PEs is partially inhibited by various more or less specific antagonists of PKCs and was therefore, in the past, almost exclusively attributed to an activating effect of β-PEs on PKCs (Majewski and Iannazzo, 1998). K^+ channels, Ca^{2+} channels, or components of the transmitter secretion apparatus such as the SNARE protein SNAP-25 and the presynaptic regulatory factor GAP-43 have been suggested as possible targets of β-PEs/PKCs in the modulation of presynaptic function (Parfitt and Madison, 1993; de Graan et al., 1994; Shimazaki et al., 1996; Redman et al., 1997; Hoffman and Johnston, 1998; Minami et al., 1998; Stevens and Sullivan, 1998; Hori et al., 1999; Yawo, 1999a, 1999b; Honda et al., 2000; Oleskevich and Walmsley, 2000; Oleskevich et al., 2000; Waters and Smith, 2000).

Although published studies on the role of PKCs in presynaptic function were almost entirely based on pharmacological manipulations using β-PEs and PKC inhibitors, the concept that PKCs are important physiological mediators of enhanced neurotransmitter output with a role in transient and long-term potentiation of synaptic strength has become generally accepted. However, β-PEs and many other pharmacological tools used to modify PKC function interact equally well with other β-PE receptors (Betz et al., 1998), and several studies suggest the presence of alternative β-PE receptors with a regulatory role in neurotransmitter release (Stevens and Sullivan, 1998; Honda et al., 2000; Hori et al., 1999; Redman et al., 1997; Iwasaki et al., 2000; Waters and Smith, 2000). The best candidates for alternative presynaptic β-PE receptors belong to the family of Munc13 proteins, which constitute a family of three homologs of *Caenorhabditis elegans* Unc-13, Munc13-1, -2, and -3

[6] Correspondence: crosenm@gwdg.de, brose@em.mpg.de
[7] These authors contributed equally to this work.
[8] Present address: Department of Molecular Biology, Princeton University, Princeton, New Jersey 08544.
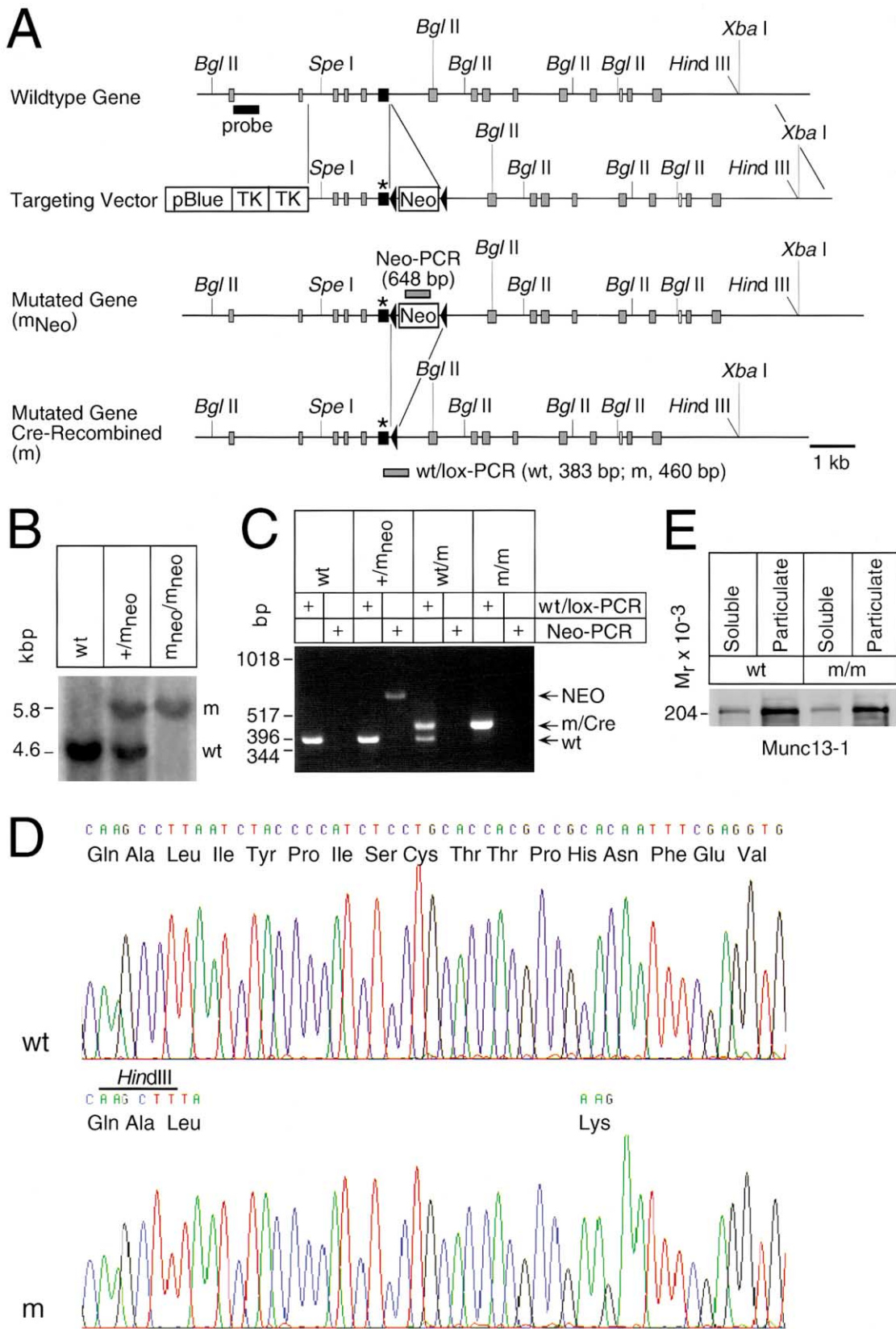
Figure 1. Strategy for the Generation of the Munc13-1^{H567K} Mutation in Mouse Embryonic Stem Cells and Basic Characterization of Homozygous Mutant Mice

(A) Wild-type Munc13-1 gene (wt), targeting vector, mutated gene after homolgous recombination (m$_{Neo}$), and mutated gene after Cre recombina-

(Brose et al., 1995). Munc13-1, the best-characterized family member, is specifically localized to presynaptic active zones (Betz et al., 1998), where it primes synaptic vesicles to fusion competence by unfolding or "activating" Syntaxin and thereby promoting core complex formation (Augustin et al., 1999b; Brose et al., 2000; Richmond et al., 2001). Thus, Munc13-1 is a β-PE receptor whose subcellular localization and function establish it as a potential target of the DAG second messenger pathway that may act in parallel with PKCs to enhance neurotransmitter release (Betz et al., 1998). Genetic studies in *C. elegans* demonstrated that a specific presynaptic regulatory pathway involving cholinergic and serotonergic control of motor neurons employs DAG and depends on Unc-13 (Lackner et al., 1999; Miller et al., 1999; Nurrish et al., 1999). These genetic interactions and data obtained in heterologous expression systems (Betz et al., 1998) led to the idea that Munc13 proteins and their homologs may be presynaptic targets for DAG in vivo.

We determined the relative contribution of PKCs and Munc13-1 to the β-PE-dependent enhancement of neurotransmitter release and to dynamic changes in synaptic efficacy using hippocampal neurons from genetically modified mice that express a β-PE binding-deficient Munc13-1^{H567K} variant instead of the wild-type protein.

Results

Basic Characterization of Mice with a H567K Point Mutation in the Munc13-1 Gene

Mice with a H567K point mutation in the Munc13-1 gene, which abolishes β-PE binding by Munc13-1, were generated as described in Experimental Procedures (Figure 1). Like Munc13-1 deletion mutants, homozygous mutant/Cre-recombined Munc13-1^{H567K}/Munc13-1^{H567K} mice (m/m) were not viable. However, they expressed Munc13-1^{H567K} at levels comparable to those of Munc13-1 in wild-type littermates (Figure 1E). Thus, intronic insertion of the remaining *loxP* site does not interfere with mRNA synthesis, splicing, or stability, and the H567K mutation does not lead to misfolding or destabilization of Munc13-1 protein. The ratio of soluble to membrane bound Munc13-1 was not altered in Munc13-1^{H567K}/Munc13-1^{H567K} mutants (Figure 1E), indicating that DAG binding by Munc13-1 is not responsible for its tight association with the cytoskeletal matrix. Like Munc13-1 deletion mutants, newborn m/m mice initially breathe, react to tactile stimuli, and exhibit pain-avoidance reflexes,

but they deteriorate rapidly and die within 2–3 hr after birth, indicating a general brain stem malfunction. The overall structure and cytoarchitecture of brains and the distribution of the synaptic marker synaptophysin in m/m mutants were indistinguishable from wild-type littermates (data not shown). Heterozygous Munc13-1^{H567K} mutants (m$^{+/+}$) were identical to wild-type controls in all analyses (data not shown), demonstrating that the Munc13-1^{H567K} protein has no dominant-negative effect.

Spontaneous and Evoked Synaptic Transmission in Munc13-1^{H567K}/Munc13-1^{H567K} (m/m) Mutants

To examine the functional consequences of destruction of the DAG/β-PE binding site in m/m mutants, we performed patch clamp analyses of individual hippocampal neurons in microisland cultures. We concentrated on glutamatergic neurons because Munc13-1 function is essential for these but not for GABAergic cells (Augustin et al., 1999b). In these cultures, presynaptic targeting of Munc13-1^{H567K} is indistinguishable from that of wild-type Munc13-1, as determined by double labeling of cultured hippocampal neurons with antibodies to Munc13-1 and Synaptophysin (Figure 2).

Routinely, cells from m/m mutants were analyzed 12–20 days after plating and compared to wild-type control cells obtained from littermates. In some experiments, we employed Munc13-1/Munc13-2 double-deficient neurons as model cells to study the characteristics of the Munc13-1^{H567K} variant in comparison to wild-type Munc13-1 following overexpression using the Semliki-Forest-Virus system. In contrast to Munc13-1-deficient glutamatergic hippocampal neurons, which still show measurable glutamate release (10% of wild-type levels; Augustin et al., 1999b), double-homozygous Munc13-1/Munc13-2-deletion mutant neurons completely lack spontaneous and evoked transmitter release but can be rescued by reintroduction of Munc13 proteins (Rosenmund et al., 2002). Autaptic responses were obtained by brief (1–2 ms) somatic depolarization, which induces an unclamped action potential that is followed by a postsynaptic response with a delay of 2–4 ms.

Although the perinatally lethal phenotype of m/m mice is similar to that of Munc13-1-deletion mutants, their electrophysiological characteristics were strikingly different. In contrast to Munc13-1-deficient neurons, m/m cells produced robust evoked EPSC amplitudes that were only slightly smaller than but not statistically different from wild-type values (4.87 $\pm$ 0.45 nA, n = 91, m/m; 5.8 $\pm$ 0.7 nA, n = 83, wild-type; Figure 3A). Likewise,

---

tion (m). Exons are indicated by black (C$_1$ domain) or gray (all other) boxes. Black triangles indicate *loxP* sites. Asterisk indiates H567K mutation. Black horizontal bar indicates probe used for Southern analysis (*Bgl* II-digested tail DNA) of mutated genes in mice. Products of diagnostic PCR reactions (size in brackets) are indicated by horizontal gray bars. Abbreviations are as follows: Neo, neomycin resistance gene; pBlue, pBluescript KS; and TK, herpes simplex virus thymidine kinase.

(B) Southern blot analysis of mutated genes using *Bgl* II-digested mouse tail DNA and the probe indicated in (A). Abbreviations are as follows: m$_{Neo}$, mutated gene; and wt, wild-type.

(C) PCR analysis of indicated phenotypes using the PCR strategy depicted in (A). Abbreviations are as follows: m, mutated gene after Cre recombination; m$_{Neo}$, mutated gene; and wt, wild-type.

(D) Sequence analysis of PCR products obtained with the wt/lox PCR depicted in (A) and (C) using mouse tail DNA as template. Abbreviations are as follows: wt, wild-type; and m, mutated gene after Cre recombination.

(E) Western blot analysis of brain homogenates from wild-type (wt) and Munc13-1^{H567K}/Munc13-1^{H567K} (m/m) mice. Soluble and particulate fractions were separated by centrifugation at 300,000 $\times$ g for 10 min. Proteins were separated by SDS-PAGE and immunoblotted for Munc13-1 using a specific monoclonal antibody to the C terminus of the protein.
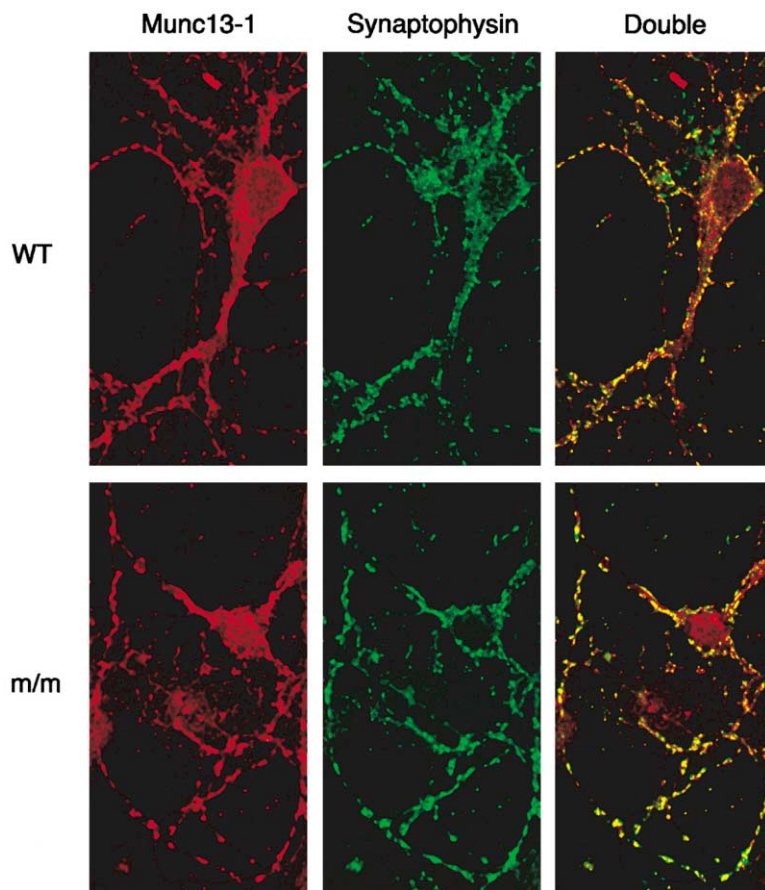
Munc13-1 Synaptophysin Double

Figure 2. Subcellular Distribution of Munc 13-1^{H567K}

Single-scan confocal image of hippocampal primary cultures from wild-type (wt) and homozygous m/m mice (m/m) that were double labeled for Munc13-1 (Alexa 568-conjugated secondary antibody, red) and the presynaptic marker Synaptophysin (Alexa 488-conjugated secondary antibody, green). The overlay image (right) shows that, irrespective of the genotype, Munc13-1 labeling coincided largely with Synaptophysin labeling. This demonstrates that Munc13-1^{H567K}, like wild-type Munc13-1, is targeted to presynaptic terminals.

mean frequency (3.7 ± 1.3 Hz, n = 10, m/m; 4.2 ± 1.9 Hz, n = 12, wild-type), amplitude (23.2 ± 1.4 pA, n = 10, m/m; 24.5 ± 1.3 pA, n = 12, wild-type), and charge (92 ± 7 pC, n = 10, m/m; 96 ± 4 fC, n = 12, wild-type) of spontaneous responses were not different between m/m and wild-type neurons. In a separate set of experiments, we found that evoked EPSC amplitudes from Munc13-2-deficient cells that express Munc13-1 as the only Munc13 isoform (1.32 ± 0.27 nA, n = 17) were indistinguishable from responses measured in Munc13-1/Munc13-2 double-deficient neurons overexpressing Munc13-1^{H567K} (1.51 ± 0.3 nA, n = 21) (Figure 3B). Thus, inactivation of the DAG/β-PE binding site in Munc13-1 leaves the postsynaptic responsiveness of neurons unaffected and does not abolish priming of synaptic vesicles or inhibit their evoked release.

Effects of β-PEs on Munc13-1^{H567K}/Munc13-1^{H567K} (m/m) Neurons

We next examined the consequences of the Munc13-1^{H567K} mutation for β-PE-mediated effects on synaptic transmission. Wild-type neurons reacted to application of 1 μM β-phorbol dibutyrat (PDBU) for 1 min with a rapid (8 s time constant) and robust enhancement of evoked EPSC amplitudes (191% ± 17% of baseline values, n = 30). Following removal of PDBU, the synaptic amplitude returned to baseline within 3–4 min (27 s time constant; Figure 3C). In contrast, m/m neurons showed a strongly reduced sensitivity toward β-PE with application of 1

μM (PDBU), resulting in a slower (16 s time constant) and smaller increase in evoked EPSC amplitudes (131% ± 7% of baseline values, n = 34, p < 0.001 compared to wild-type control cells; Figure 3D). Control experiments showed that inactive α-PE variants, which do not bind to C$_1$ domains, had no effect on evoked EPSCs in both wild-type (n = 9) and m/m neurons (n = 12). Because numerous reports showed β-PE-dependent increases in mEPSC frequency, we examined the effect of 1 μM PDBU on mEPSC frequency in control and m/m neurons. We found that in wild-type neurons, the mEPSC frequency increased to 239% ± 34% (n = 8) of control levels, while in m/m cells a much weaker increase was observed (127% ± 16% of control levels, n = 7). These data provide direct evidence that Munc13-1 is the main presynaptic target for β-PE-mediated enhancement of synaptic transmitter release in hippocampal neurons.

Although dramatically reduced in comparison to the wild-type situation, β-PE-mediated enhancement of spontaneous and evoked synaptic transmitter release was still detectable in m/m neurons (Figure 3D). To test whether this is due to the presence of Munc13-2 (the only Munc13 isoform coexpressed with Munc13-1 in glutamatergic hippocampal nerve cells [Augustin et al., 1999a, 2001]), we overexpressed wild-type Munc13-1 or Munc13-1^{H567K} in Munc13-1/Munc13-2 double-deficient neurons using the Semliki-Forest-Virus system and tested their sensitivity to β-PEs. Similar to wild-type
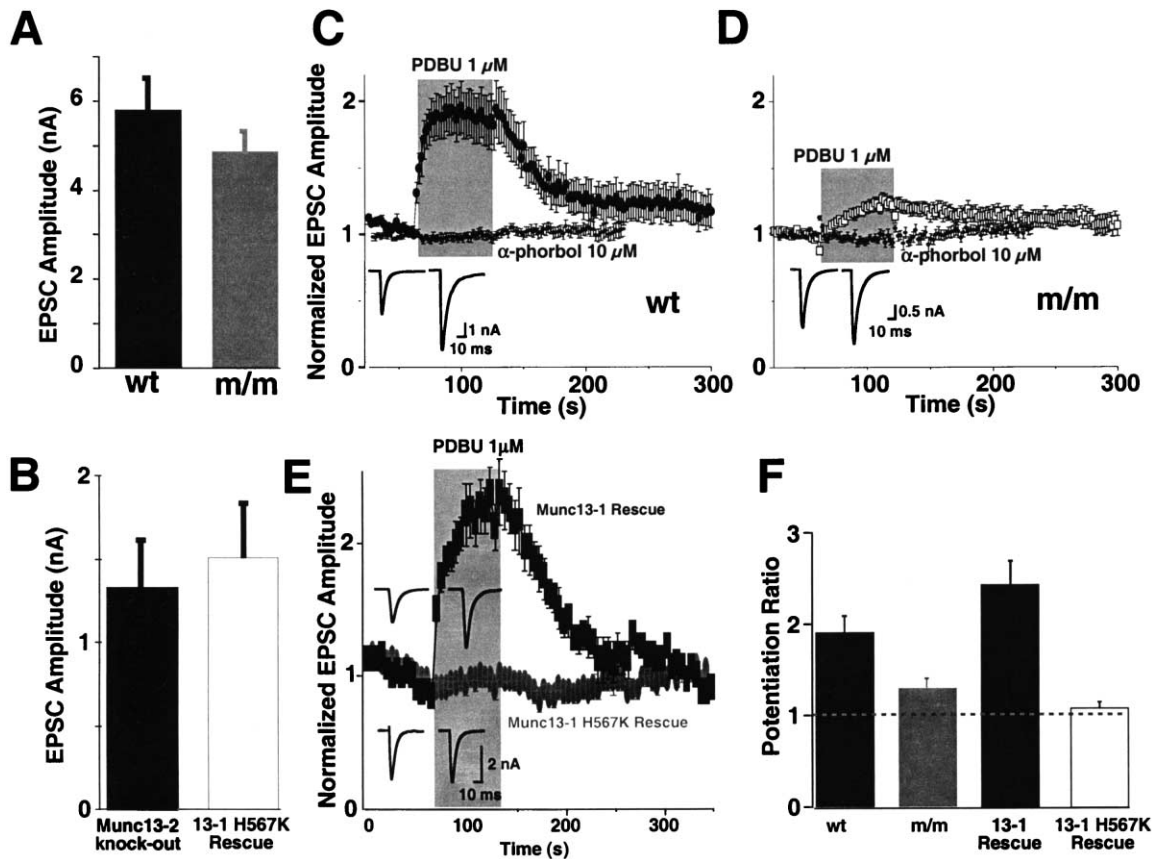
Figure 3. Effects of the Munc13-1[H567K] Mutation on Synaptic Responses and Their β-PE-Mediated Potentiation

(A) Evoked excitatory autaptic currents from wild-type (n = 83) and m/m (n = 91) neurons. Error bars indicate standard error of mean.

(B) Synaptic currents from Munc13-2-deficient (n = 17) and Munc13-1/Munc13-2 double-deficient cells overexpressing Munc13-1[H567K] (n = 21). Error bars indicate standard error of mean.

(C and D) Time course of β-PE effects on evoked EPSCs in (C) wild-type (n = 30) and (D) m/m (n = 34) neurons. Application period (1 min) of β-PE dibutyrat (PDBU, 1 μM) or its inactive analog α-phorbol (10 μM, assayed in separate experiments) is indicated by a gray box. EPSCs were evoked at 0.5 Hz and normalized to the initial amplitude. Error bars indicate standard error of mean.

(E) Time course of β-PE effects on evoked EPSCs in Munc13-1/Munc13-2 double-deficient cells overexpressing wild-type Munc13-1 (n = 12) or Munc13-1[H567K] (n = 17). Application period (1 min) of β-PE dibutyrat (PDBU, 1 μM) is indicated by a gray box. EPSCs were evoked at 0.5 Hz and normalized to the initial amplitude. Error bars indicate standard error of mean.

(F) Average potentiation of evoked EPSC amplitude from experiments shown in (C)–(E) 30 s following onset of PDBU application. Dotted line is control amplitude. Holding potential −75 mV. Error bars indicate standard error of mean.

neurons, Munc13-1/Munc13-2 double-deficient neurons overexpressing wild-type Munc13-1 responded to application of 1 μM PDBU with a rapid and robust increase in evoked EPSCs (246% ± 22% of control levels, n = 12; Figures 3E and 3F). In contrast, Munc13-1/Munc13-2 double-deficient cells overexpressing Munc13-1[H567K] were completely insensitive to 1 μM PDBU (108% ± 5% of control levels, n = 17; Figures 3E and 3F), although evoked EPSC amplitudes were reconstituted to control levels (Figure 3B). Thus, β-PE-dependent enhancement of presynaptic transmitter release from hippocampal neurons is entirely dependent on the presence of Munc13-1 and Munc13-2.

The above results are in conflict with the widely held view that PKCs are the main β-PE targets in the presynapse. Published conclusions about the role of PKCs in the regulation of transmitter release are largely based on indirect pharmacological evidence. Data from our genetic approach, however, suggest that Munc13s and

not PKCs are responsible for the β-PE-mediated enhancement of neurotransmitter release. This view was further supported in a pharmacological analysis of wild-type hippocampal neurons. We found that the specific PKC inhibitor GÖ 6983, a bisindolylmaleimide (BIS) derivative that is thought to specifically interact with ATP binding sites of several PKCs, had no effect on the β-PE-induced increase in evoked EPSCs (160% ± 9% of baseline values, n = 10, with 1 μM PDBU alone; 150% ± 6% of baseline values, n = 10, after preincubation for 2 min and in the presence of 3 μM GÖ 6983). This shows that GÖ 6983-sensitive PKCs are not involved in the β-PE effects observed here. In addition, we examined the effects of BIS I (GÖ 6850), a widely used but somewhat less specific inhibitor of PKCs. We first treated wild-type neurons for 1 min with 1 μM PDBU and measured the induced increase of evoked EPSC amplitudes at 0.2 and 0.033 Hz stimulation frequencies (50%–60% increase over baseline, n = 7 each; Figures 4A and 4C).
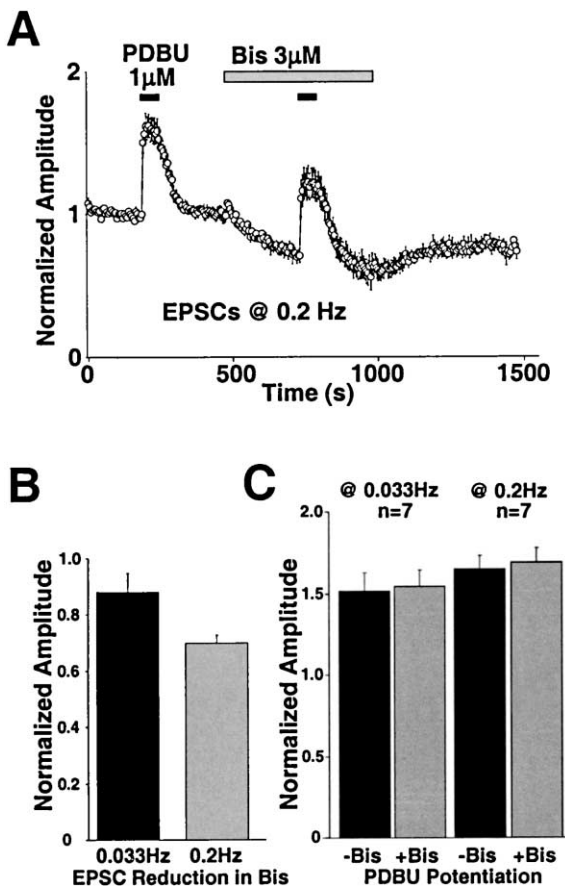
Figure 4. Pharmacology of β-PE-Induced Potentiation in Wild-Type Neurons

(A) Time course of β-PE effects on evoked EPSCs (0.2 Hz) in wild-type neurons (n = 7). Application of PDBU (1 μM) is indicated by a black bar. Application of BIS 1 (3 μM) is indicated by a gray box. Incubation of bisindoylmaleimide I led to a partially irreversible rundown of evoked EPSC amplitudes but did not block the potentiation induced by application of PDBU (1 μM) for 1 min (white box).

(B) Average evoked EPSC amplitudes after treatment with bisindoylmaleimide I (normalized to control values before drug application). Note that the degree of rundown induced by bisindoylmaleimide I is dependent on the stimulation frequency and larger at higher frequencies (n = 7 for each frequency).

(C) Average β-PE-mediated potentiation in untreated (−Bis) and bisindoylmaleimide I (3 μM) pretreated (+Bis) neurons, calculated by dividing the evoked EPSC amplitude 30 s following the application by that immediately before application of 1 μM PDBU (n = 7 for each frequency/treatment group).

Following washout of PDBU, application of BIS I (3 μM) led to a partial and irreversible rundown of evoked EPSC amplitudes. The degree of this rundown was dependent on the stimulation frequency (35% at 0.2 Hz, n = 7, and 15% at 0.033 Hz, n = 7, over a 4 min application period; Figures 4A and 4B). However, the resulting reduced evoked EPSC responses were still potentiated by application of 1 μM PDBU, and the degree of this potentiation was similar to the one observed with PDBU alone (Figures 4A and 4C). A very similar BIS I-dependent reduction of evoked EPSC amplitudes was seen in m/m neurons (data not shown), indicating that this rundown is not directly related to the function of the Munc13-1 C_1 domain. Thus, BIS I acts on evoked EPSC responses

through an unknown, possibly toxic mechanism (e.g., by influencing RRP refilling rates), but does not prevent the β-PE-induced potentiation of transmitter release.

Expression and Function of PKCs in Munc13-1[H567K]/ Munc13-1[H567K] (m/m) Neurons
In principle, the data presented so far would also be compatible with the view that the H567K point mutation in Munc13-1 influences levels or function of PKCs. To test this directly, we first examined the protein expression levels of PKCs by densitometric analysis of Western blots obtained with brain homogenates from wild-type and m/m mice. We found that protein levels of all tested PKCs were unaffected by the m/m mutation (Figures 5A and 5B). Second, we analyzed β-PE-dependent PKC activity in cultures from wild-type and m/m mutant brains. Cortical/hippocampal primary cultures were loaded with [32P]orthophosphate and stimulated with 1 μM PDBU. Labeled proteins were separated by 2D electrophoresis and visualized autoradiographically. Autoradiographs of wild-type and m/m cultures showed identical patterns of proteins that were phosphorylated in a β-PE-dependent manner (Figure 5C), demonstrating that overall β-PE-dependent PKC activity is not affected by the m/m mutation. Third, we examined the β-PE-dependent phosphorylation of two identified presynaptic targets of PKCs, SNAP-25 (Shimazaki et al., 1996) and GAP-43/B-50 (de Graan et al., 1994). We prepared cultures from wild-type and m/m brains, which were then stimulated with 1 μM PDBU, harvested, and analyzed by SDS-PAGE and Western blotting using phosphopeptide-specific antibodies (Iwasaki et al., 2000; Kawakami et al., 2000). Again, we detected no differences between the tested genotypes with respect to PKC activity. SNAP-25 and GAP-43 were strongly phosphorylated in a β-PE-dependent manner in both wild-type and m/m cultures (Figure 5D). Thus, PKC-dependent phosphorylation of synaptic targets is normal in m/m mutants. Finally, we tested whether Munc13-1 acts as a substrate for PKCs and whether PKC-dependent phosphorylation of Munc13-1 is affected by the H567K mutation. We used cortical/hippocampal primary cultures from wild-type and m/m brains, which were loaded with [32P]orthophosphate and stimulated with 1 μM PDBU. Proteins were extracted with detergent, and Munc13-1 was immunoprecipitated using a specific polyclonal antibody (Betz et al., 1997). Phosphorylated and immunoprecipitated material was separated by SDS-PAGE and analyzed by autoradiography. In parallel, aliquots of the same samples were analyzed by Western blotting for Munc13-1 and densitometric analysis. We found that Munc13-1 was weakly phosphorylated in a constitutive, β-PE-independent manner in all genotypes tested (Figure 5E). However, in wild-type and m/m brains, a β-PE-dependent phosphorylation of Munc13-1 was not observed. The ratio between immunoprecipitated and phosphorylated Munc13-1 was very similar between all genotypes and treatment groups, indicating that Munc13-1 is not a PKC target (Figure 5E).

Functional Consequences of the Munc13-1[H567K] Mutation for Synaptic Transmission
We next investigated the physiological role of DAG-dependent regulation of transmitter release and the role
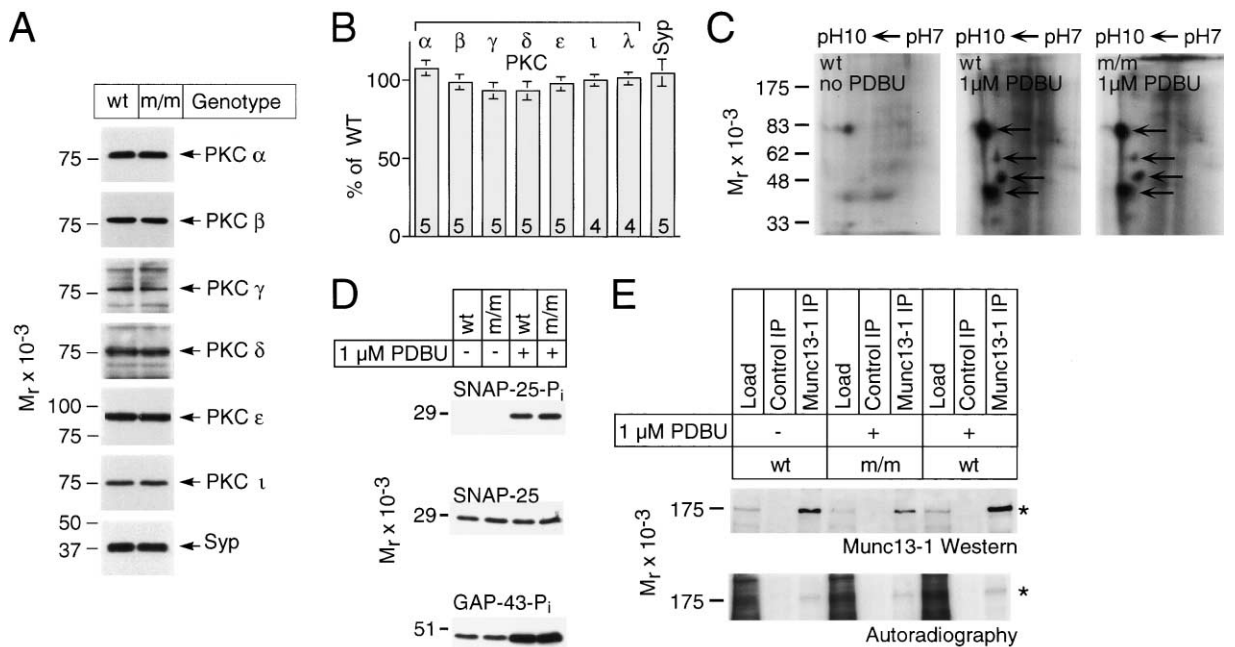
Figure 5. Expression and Function of PKCs in Munc13-1^{H567K}/Munc13-1^{H567K} (m/m) Neurons

(A) Western blot analyses of various PKCs and Synaptophysin (Syp) in brain homogenates from a wild-type (wt) and a m/m (m/m) brain.

(B) Quantitative analysis of PKC levels determined by Western blotting. Protein levels in m/m brains are expressed as % of wild-type controls. Respective n values are given at the base of histogram bars. Note that PKCλ and PKCτ are orthologs and PKCλ is not shown in (A). Syp indicates synaptophysin. Error bars indicate standard error of mean.

(C) Autoradiographs of 2D gels (selected sections) obtained from ^{32}P-labeled cultures of wild-type (wt) and m/m (m/m) brains in the absence or presence of β-PE (1 μM PDBU). Arrows indicate proteins that are specifically phosphorylated in a β-PE-dependent manner.

(D) β-PE-dependent phosphorylation of SNAP-25 and GAP-43 in wild-type (wt) and m/m (m/m) cultures. Cultures were treated as decribed in Experimental Procedures. Identical amounts of proteins were separated by SDS-PAGE and probed with specific antibodies for phosphorylated SNAP-25 (SNAP-25-P$_i$), total SNAP-25 (SNAP-25), and phosphorylated GAP-43 (GAP-43-P$_i$).

(E) Test for β-PE-dependent phosphorylation of Munc13-1. Wild-type (wt) and m/m (m/m) cultures were labeled with [^{32}P]orthophosphate and stimulated with 1 μM PDBU. Proteins were extracted and Munc13-1 was immunoprecipitated using specific polyclonal antibodies (Munc13-1 IP) or control preimmune serum (Control IP). Immunoprecipitated material as well as the extract before precipitation (Load) were separated by SDS-PAGE. Labeled proteins were visualized by autoradiography. Immunoprecipitated Munc13-1 was detected by immunoblotting with a specific monoclonal antibody. Asterisks indicate Munc13-1 bands.

of Munc13-1 in this process by examining RRP sizes and release dynamics in m/m and wild-type control cells. We determined RRP size by quantifying the transient burst of exocytotic activity following application of hypertonic sucrose solution (Stevens and Tsujimoto, 1995; Rosenmund and Stevens, 1996). The RRP was significantly smaller in m/m neurons (0.58 ± 0.11 nC or 6373 ± 660 vesicles, n = 81) than in wild-type control cells (1.04 ± 0.11 nC or 10947 ± 1157 vesicles, n = 72, p < 0.001) (Figure 6A). However, using a paired pulse stimulation paradigm with consecutive hypertonic sucrose pulses at variable interpulse intervals, we found that the rate by which the RRP was refilled after complete depletion was unaffected by the m/m mutation (Figure 6B).

Unaltered evoked EPSC amplitudes (Figure 3A) together with reduced RRP size (Figure 6A) indicate an increase in the average vesicular release probability P$_{vr}$ in m/m cells. Calculated P$_{vr}$, obtained by dividing the quantal content of the average evoked EPSC by the RRP size, was 10.5% ± 0.8% (n = 81) for m/m and 6.9% ± 0.6% (n = 72) for wild-type cells (p < 0.001, Figure 6C). Similar increases in P$_{vr}$ over wild-type control cells were observed in Munc13-1/Munc13-2 double-deficient neurons overexpressing Munc13-1^{H567K} (Figure

6C), indicating that increased P$_{vr}$ is a consequence of the Munc13-1^{H567K} mutation. To investigate how this P$_{vr}$ increase in m/m cells affects the synaptic release probability P$_r$, we estimated P$_r$ by analyzing the use-dependent, progressive block of NMDA-EPSCs in the presence of MK-801, which reflects the release probability across all synapses of a given neuron (Rosenmund et al., 1993, Hessler et al., 1993). This method samples most glutamatergic synapses, including silent synapses that are not contributing to AMPA-mediated EPSCs. Control and m/m cells showed a similar initial fast decay of EPSC amplitudes as a function of stimulus number, while the slower component of the EPSC decay appeared to be somewhat, but not significantly, smaller in m/m cells (Figure 6D).

The shift in release probabilities observed in m/m mutant neurons is predicted to have consequences for synaptic short-term plasticity and transmission during high-frequency stimulation. We therefore monitored the stability of evoked EPSCs at action potential frequencies of 1–10 Hz. Compared to wild-type responses, evoked EPSC amplitudes of m/m neurons showed more pronounced depression (steady-state versus initial amplitude of the train) at all frequencies tested (Figures 7A–7C). This aberrant synaptic depression during high-frequency stimulation,
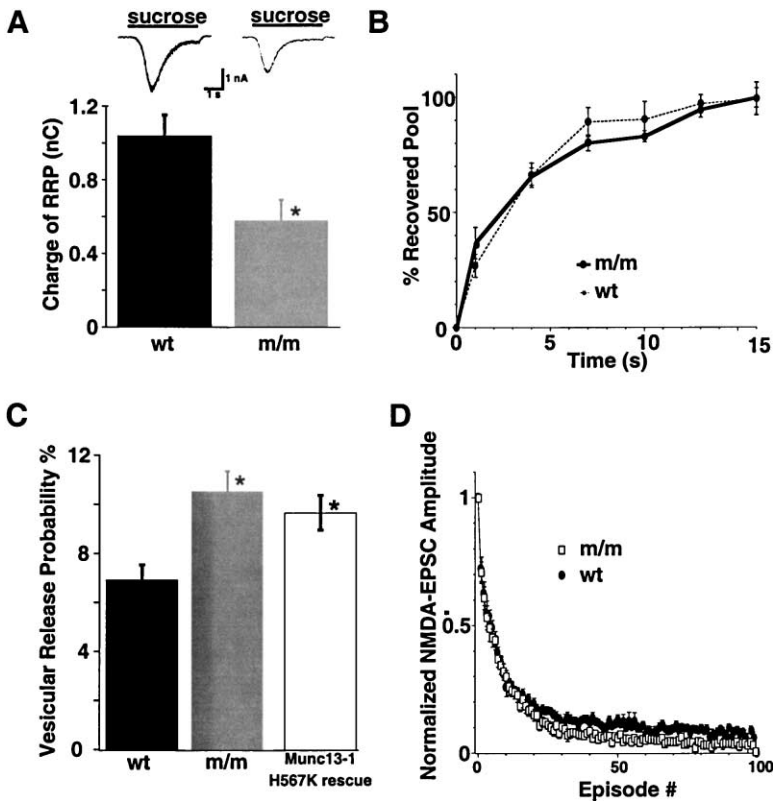
Figure 6. Readily Releasable Vesicle Pool and Release Probability in Wild-Type and Munc13-1[H567K]/Munc13-1[H567K] (m/m) Neurons

(A) Example traces of responses (top) and average transient charge component (bottom) of release of the readily releasable vesicle pool in glutamatergic neurons induced by hypertonic sucrose solution (500 mOsm hypertonic, 4 s). Asterisk indicates significant reduction ($p < 0.001$) of the readily releasable vesicle pool in m/m (n = 81) over wild-type control neurons (n = 72).

(B) Refilling kinetics of the readily releasable vesicle pool under resting conditions as measured in a paired pulse protocol consisting of two 4 s applications of hypertonic solution at varying interpulse intervals. The transient charge component of the second response was divided by the first response.

(C) Average vesicular release probability P_{vr} of wild-type (n = 72) and m/m neurons (n = 81) as well as Munc13-1/Munc13-2 double-deficient neurons overexpressing Munc13-1[H567K] (rescue; n = 17) was calculated by dividing the evoked EPSC charge by the charge of the response following depletion of the readily releasable vesicle pool with hypertonic solution. Asterisks indicate significant increase ($p < 0.01$) of P_{vr} over wild-type control neurons.

(D) Synaptic release probability as determined by NMDA-EPSC amplitude decay during ongoing EPSC stimulation in the presence of the irreversible NMDA open channel blocker MK-801 (5 μM). EPSC amplitude was normalized to the first response in the presence of MK-801. External solution contained 2.7 mM Ca^{2+}, no Mg^{2+}, and 10 μM glycine. Stimulation frequency was 0.33 Hz.

which was already detectable with the second stimulus, was even more pronounced when we tested characteristics of Munc13-1[H567K] after Semliki-Forest-Virus-mediated overexpression on the Munc13-1/Munc13-2 double-deletion background. Synaptic depression at 10 Hz stimulation frequency in Munc13-1/Munc13-2 double-mutant cells overexpressing wild-type Munc13-1 was comparable to that seen in wild-type cells (Figures 7B and 7D). In contrast, Munc13-1/Munc13-2 double-mutant neurons overexpressing Munc13-1[H567K] showed a degree of synaptic depression that even exceeded that of m/m mutant neurons (Figure 7D), most likely because the contribution of wild-type Munc13-2 is lacking in these cells.

Our data on m/m neurons obtained with high-frequency stimulation paradigms demonstrate that an intact C_1 domain in Munc13-1 is essential for the maintenance of high levels of transmitter release during high-frequency action potential trains. However, we already showed that the refilling rate of the RRP as determined by responses to paired hypertonic sucrose pulses (i.e., in the absence of activity) is normal in m/m neurons (Figure 6B). We examined a possible role for the Munc13-1 C_1 domain in activity-dependent refilling of the RRP using two experimental paradigms. First, we depleted the RRP by a 40 Hz/2.5 s stimulation train and determined the recovery rate of the evoked EPSC amplitude (i.e., the refilling rate of the RRP) by measuring the EPSC response to a single stimulus given at different time intervals after the

end of the 40 Hz train (Figure 8A). We found that m/m neurons recovered more slowly from RRP depletion than wild-type cells (τ = 1.52 s, n = 8, in m/m cells versus τ = 0.81 s, n = 12, in wild-type cells; Figure 8A). Second, we continuously stimulated neurons at 10 Hz and intermittently depleted the RRP with a hypertonic sucrose pulse (4 s; Figure 8B). Following return to normal osmolarity, the EPSC amplitude returned to a steady-state amplitude within seconds. We first analyzed the time course of this recovery. Both m/m neurons (τ = 0.88 ± 0.09 s, n = 36, p = 0.015) and Munc13-1/Munc13-2 double-deficient neurons overexpressing Munc13-1[H567K] (τ = 0.93 ± 0.10 s, n = 14, p = 0.015) showed a significantly slower recovery time constant than wild-type neurons (τ = 0.61 ± 0.047 s, n = 29; Figure 8C). As a more direct measure of the activity-dependent refilling kinetics, we determined the initial slope of recovery following return to normal osmolarity, which represents the rate by which new vesicles arrive. To allow direct comparison of RRP refilling between cells, we expressed this rate in pool units/second by normalizing EPSC responses during recovery to the initial EPSC amplitude at the beginning of the train (defined as 1 pool unit). Both m/m neurons (0.13 ± 0.01 pool units/ s, n = 36, p < 0.001) and Munc13-1/Munc13-2 double-deficient neurons overexpressing Munc13-1[H567K] (0.059 ± 0.01 pool unit/s, n = 14, p < 0.001) had strongly reduced refilling kinetics compared to wild-type cells (0.29 ± 0.027
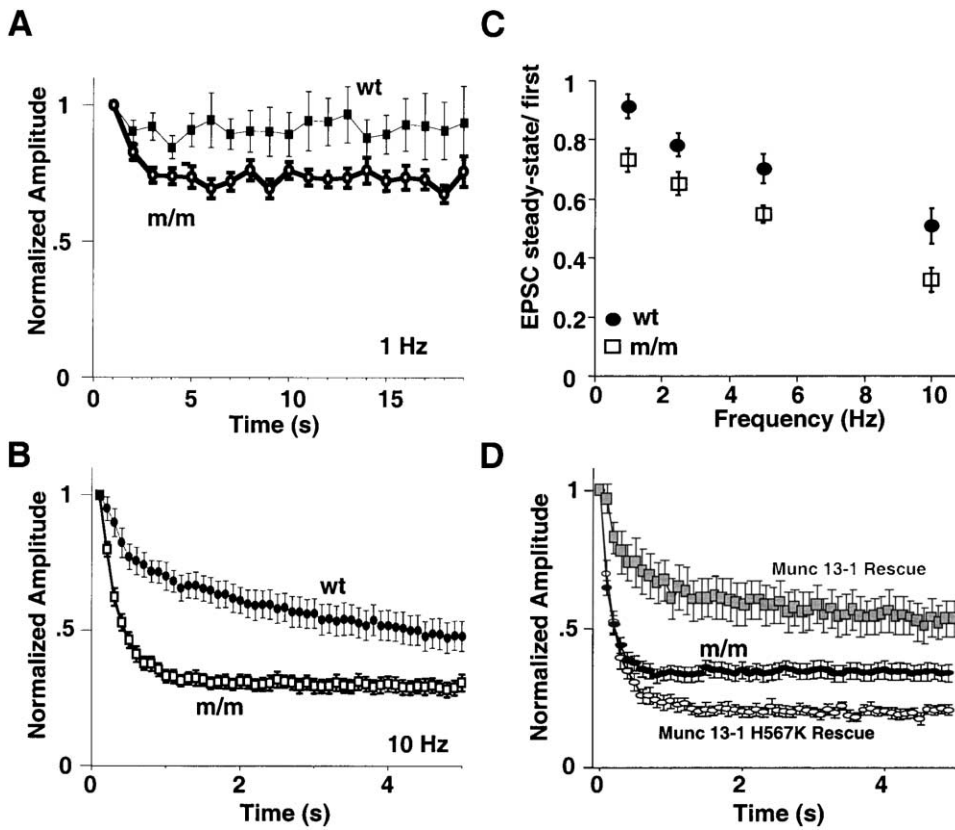
Figure 7. Release Dynamics in Wild-Type and Munc13-1[H567K]/Munc13-1[H567K] (m/m) Neurons

(A and B) Normalized evoked EPSC amplitudes of wild-type (n = 8) and m/m neurons (n = 16) at (A) 1 Hz and (B) 10 Hz stimulation rates.

(C) Depression of EPSC amplitudes during action potential trains of 1, 2.5, 5, and 10 Hz as calculated from steady-state amplitude divided by first amplitude of the train (n = 6–8 for wild-type and n = 15–16 for m/m neurons).

(D) Comparison of 10 Hz depression time course between m/m neurons (black circles; n = 19) and Munc13-1/Munc13-2 double-deficient neurons overexpressing wild-type Munc13-1 (gray squares; n = 13) or Munc13-1[H567K] (open circles; n = 19). Note that depression is less pronounced in the m/m neurons, presumably because of a remaining fraction of synapses that employ Munc13-2.

pool unit/s, n = 29; Figure 8D). Thus, Munc13-1 participates in the activity-dependent refilling of the RRP, with its C_1 domain acting as an activity sensor.

Discussion

β-PE-Mediated Enhancement of Transmitter Release: Munc13s versus PKCs

The most striking conclusion of the present study is that in hippocampal neurons, Munc13s and not PKCs are the only receptors involved in the acute regulation of presynaptic transmitter release by β-PEs or DAG. This view is based on three key findings First, mutant m/m neurons exhibit a dramatic reduction in β-PE sensitivity of transmitter release (Figures 3C and 3D). This reduction is complete when the contribution of wild-type Munc13-2 is abolished (Figures 3E and 3F). Second, expression and β-PE-dependent activity of PKCs are normal in m/m neurons (Figure 5). Therefore, the consequences of the Munc13-1[H567K] mutation are not due to an indirect effect on PKCs. Third, Munc13-1 is not a PKC substrate (Figure 5) and therefore unlikely to act as a downstream effector of PKCs. Thus, the consequences of the Munc13-1[H567K] mutation are not due to

the disruption of a hypothetical signaling cascade that is initiated by PKCs and propagated by Munc13s.

This conclusion is in conflict with most published views of PKC function in the control of neurotransmitter release. However, many previously published data indicating a role for PKCs in the regulation of transmitter release are equally compatible with alternative interpretations. Most published PKC studies depended on pharmacological tools whose specificity is still poorly characterized. We found here that BIS I/GÖ 6850, one of the most frequently used "PKC-specific" drugs, inhibits neurotransmission even in the absence of β-PEs (Figure 4). This effect compromises the use of this drug as a pharmacological tool. Moreover, an alternative PKC inhibitor, GÖ 6983, had no effect on the β-PE-induced increase in transmitter secretion studied here. Thus, published pharmacological data on the role of PKCs in the regulation of transmitter release have to be interpreted with care. Indeed, the only case where an alternative approach was taken (genetic deletion of PKCγ in mice; Goda et al., 1996) gave no evidence for an involvement of PKCs in the regulation of transmitter release, and several studies indicate the presence of alternative functional β-PE receptors in the presynapse because β-PE
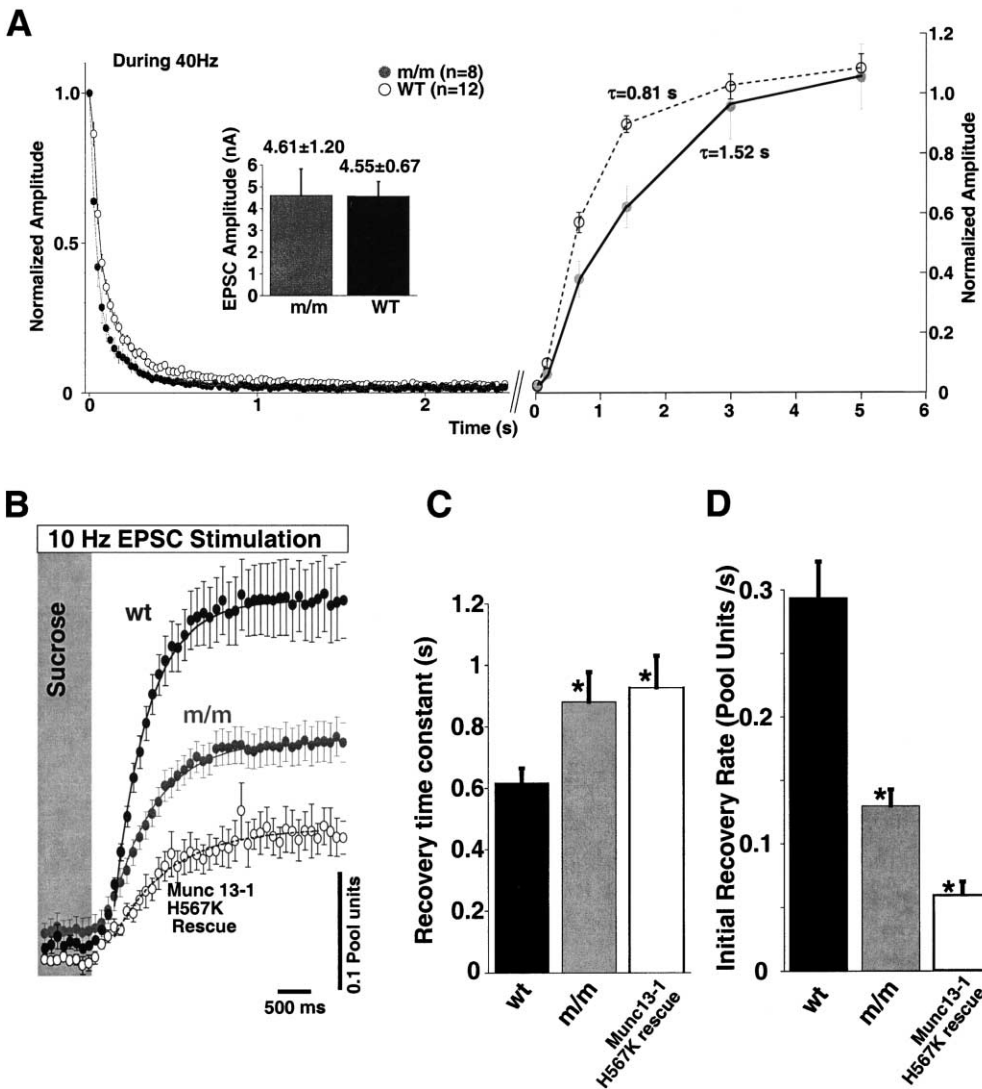
Figure 8. Activity-Dependent Refilling of Readily Releasable Vesicle Pools in Munc13-1[H567K]/Munc13-1[H567K] (m/m) Neurons

(A) Recovery of evoked EPSC amplitudes following depletion of the pool by a 2.5 s/40 Hz stimulation train. A 2.5 s train of 40 Hz stimulation was applied to excitatory cells in order to deplete the readily releasable vesicle pool (left). Single stimuli were then given at different intervals after the train in order to determine the time course of recovery of the evoked EPSC response to pretrain baseline values (right; all amplitude values are normalized to the pretrain baseline). Note that EPSC amplitudes in m/m neurons recover more slowly from pool depletion ($\tau =$ 1.52 s) than under wild-type conditions ($\tau = 0.81$).

(B) Recovery of evoked EPSC amplitudes following depletion of the pool by hypertonic sucrose application during ongoing 10 Hz stimulation. A train of 10 Hz was applied to excitatory cells. After 5 s of stimulation at 10 Hz (data not shown), the readily releasable vesicle pool was intermittendly depleted by an application of hypertonic solution for 4 s (gray bar), and the recovery of the synaptic response during ongoing 10 Hz stimulation was monitored for another 10–20 s. Shown are average evoked EPSC amplitudes of wild-type (black circles; n = 29) and m/m cells (gray circles; n = 36), as well as of Munc13-1/Munc13-2 double-deficient neurons overexpressing Munc13-1[H567K] (open circles; n = 14) as they recover from depletion upon return to normal osmolarity. The amplitudes were normalized to the initial EPSC amplitude in the train. It was assumed that the initial amplitude results from a fully filled readily releasable vesicle pool (1 pool unit).

(C) Time constants of recovery of evoked EPSC amplitudes following removal of hypertonic solution, calculated by an exponential fit of data set in (B). Values of n as in (B). Asterisks indicate significant change compared to wild-type cells (p = 0.015). Note that the recovery time constant is also influenced by the rate of depletion.

(D) Initial slope of recovery of evoked EPSC amplitudes following return to normal osmolarity, calculated from data set shown in (B). Values of n as in (B). Asterisks indicate significant change compared to wild-type cells (p = 0.015).

effects were not completely reversed by PKC inhibitors (Stevens and Sullivan, 1998; Honda et al., 2000; Hori et al., 1999; Redman et al., 1997; Iwasaki et al., 2000; Waters and Smith, 2000). In the most striking example (Iwasaki et al., 2000), β-PE-mediated effects on protein phosphorylation by PKCs and secretion in PC12 cells

were shown to be distinct with respect to time course, dependence on β-PE concentration, and sensitivity to PKC inhibitors and less-specific kinase blockers.

Our data only allow conclusions about the relative importance of Munc13s and PKCs in the control of neurotransmitter release from hippocampal neurons. How-

ever, in view of the present study and the fact that ubMunc13-2 is also expressed in nonneuronal tissues (Song et al., 1998; Betz et al., 2001), a reevaluation of reported PKC-mediated effects in nonneuronal tissues is required. Evidence for functional non-PKC β-PE receptors in more general processes such as protein export from the ER has already been provided (Fabbri et al., 1994).

Regulation of Munc13-1 Function via the C_1 Domain

Analyses of release and pool dynamics in m/m neurons revealed a surprising insight into the function of the Munc13-1 C_1 domain. We found that the RRP size was reduced in m/m neurons under resting conditions (Figure 6A), but activity-independent refilling of the RRP was normal (Figure 6B). Thus, the m/m mutation does not simply cause a retardation of RRP refilling rates in the resting state. In addition, we observed that evoked EPSC amplitudes were hardly affected in m/m neurons (Figure 3A) despite an underlying reduction in the size of the RRP (Figure 6A), indicating that the remaining vesicle pool has an intrinsically higher vesicular release probability (P_{vr}) than the average release probability in neurons with an intact Munc13-1 C_1 domain. This effect of the m/m mutation on P_{vr} has striking consequences for the activity-dependent regulation of transmitter release, since it leads to aberrant synaptic depression during trains of action potentials (Figure 7) and retarded refilling of RRPs during/after high-frequency stimulation (Figure 8). These findings indicate that Munc13-1, in addition to mediating basal synaptic vesicle priming (Augustin et al., 1999b), participates in the maintenance of RRPs during high-action potential frequencies. High-frequency stimulation appears to cause Ca^{2+} influx, activation of phospholipase C, and transient increases in synaptic levels of DAG, which in turn binds to the C_1 domain of Munc13-1 and boosts its priming activity. The fact that m/m mice die immediately after birth indicates that the C_1 domain-dependent stimulation of Munc13-1 activity and the concomitant adaptation to high-activity levels may be important for neurons involved in essential body functions (e.g., rhythmically active nerve cells in the respiratory system).

It is unclear how Munc13-1 via its C_1 domain regulates P_{vr} and the refilling of the RRP in an activity-dependent manner. Munc13-1 binding to its putative substrate Syntaxin is not affected by β-PEs (A.B. and N.B., unpublished data). One possibility is that wild-type hippocampal neurons, like other cells (Voets, 2001; Sakaba and Neher, 2001a, 2001b), form two functionally distinct pools of releasable vesicles. One pool is reluctantly releasable (low P_{vr}) but quickly replenished and contributes only weakly to action potential-induced release at low-stimulation frequencies. Processes such as ongoing synaptic activity or direct activation of the Munc13-1 C_1 domain increase the size of or facilitate release from this low P_{vr} pool. The m/m mutation abolishes it, resulting in an apparent increase in average P_{vr}. The other pool is readily releasable (high P_{vr}) but slowly replenished, is the main contributor to evoked release at low-stimulation frequencies, is unaffected in m/m cells, and thus, is independent of Munc13-1 C_1 domain function. This

two-pool model would explain why m/m neurons show increased P_{vr}, i.e., normal EPSC amplitudes, despite reduced RRPs. The observed increases in paired pulse depression and synaptic depression rate at 1–10 Hz stimulation frequencies and lower steady-state amplitudes during trains of stimuli (Figure 7) are predicted consequences of the increased apparent P_{vr} seen in m/m neurons. The reduced activity-dependent refilling rates in m/m neurons (Figure 8) can be explained by a lack of "activation" of the low P_{vr} pool for secretion by high-frequency stimulation or β-PEs.

A molecular model of how Munc13-1 activity may define two different pools of releasable vesicles can be inferred from the mechanism of DAG-dependent membrane recruitment of PKCs. Munc13-1 is present in a soluble pool and in a pool that is tightly associated with the cytoskeletal matrix of the presynaptic active zone by a proteinaceous linker (Figure 1E; Betz et al., 2001), and soluble Munc13-1 can translocate to the plasma membrane in a β-PE-dependent manner (Betz et al., 1998; Ashery et al., 2000). The insoluble, active zone resident Munc13-1 pool may define the pool of slowly refilling, high P_{vr} vesicles because it is functionally integrated into the release machinery of the active zone and has access to all necessary regulatory proteins (Betz et al., 2001). In contrast, the pool that is dependent on the Munc13-1 C_1 domain and characterized by fast refilling rates but low P_{vr} may be generated by Munc13-1 molecules that have been recruited from the cytosol to the presynaptic plasma membrane in a DAG-dependent manner. These recruited, nonactive zone resident Munc13-1 molecules could represent "ectopic" priming sites that are partially functional but lack active zone-specific regulatory components, hence their fast refilling rate and low P_{vr}. In the absence of stimulation, the number of ectopic priming sites would be dependent on the resting DAG level in the presynaptic active zone plasma membrane. Tonically present ectopic priming sites would be largely eliminated in m/m neurons, leading to a reduction in the size of the readily releasable vesicle pool (Figure 6A). The number of ectopic sites would be increased by activity-dependent increases in membrane DAG levels or by β-PEs, which indeed cause increases in the size of the readily releasable vesicle pool (Stevens and Sullivan, 1998).

Currently, the endogenous transmitter systems and signal transduction pathways that target Munc13s in the mammalian brain are unknown. The main task of future studies will be to identify and characterize endogenous transmitter and second messenger systems that control Munc13 function by regulating DAG levels.

Experimental Procedures

Stem Cell Experiments

A previously published mouse genomic clone (pM13-27.1; Augustin et al., 1999b) was used to construct a targeting vector for the generation of Munc13-1[H567K] mutant mice by homologous recombination in embryonic stem cells (Figure 1A). In the targeting vector, a Neomycin resistance gene flanked by two *loxP* sites was inserted in antisense orientation into an intronic sequence between a short arm with the exon encoding the Munc13-1 C_1 domain and a long arm with about 8 kb of genomic sequence containing multiple exons. In addition, two copies of the HSV thymidine kinase gene were attached 5' to the short arm for negative selection. The short arm was generated

by PCR using the mouse genomic sequence as template and designed to contain three point mutations, one silent to generate a *Hin*d III site for diagnostic purposes, and two to generate the H567K mutation (Figure 1D). Mice carrying the mutated Munc13-1[H567K]/Neo gene (m_{neo}) were generated as described (Augustin et al., 1999b) and identified by Southern blotting (Figures 1A and 1B). Once homologous recombination and germline transmission of the mutation had been verified, mice were routinely genotyped by PCR (Figures 1A and 1C). Like Munc13-1-deletion mutants (Augustin et al., 1999b), animals homozygous for the mutated Munc13-1[H567K]/Neo gene (m_{neo}/m_{neo}) were not viable and contained no Munc13-1[H567K] protein (data not shown), most likely because the integration of the Neomycin resistance gene in antisense orientation into the intronic sequence flanking the C_1 domain exon compromises Munc13-1 mRNA synthesis or splicing. To eliminate deleterious effects of the Neomycin resistance gene, we crossed heterozygous mice carrying the mutated Munc13-1[H567K]/Neo gene (+/m_{neo}) with EIIa-*cre* mice, which carry the *cre* transgene under the control of the adenovirus EIIa promoter and express Cre recombinase in early embryonic stages (Lakso et al., 1996). Successfully recombined genes (Munc13-1[H567K]) in offspring from these interbreedings were genotyped by PCR/restriction digestion and tested for germline transmission (Figures 1A and 1C). Genomic integration of the point mutations was verified by sequencing of the PCR products (Figure 1D). In all experiments, wild-type and Munc13-1[H567K]/Munc13-1[H567K] (m/m) mutant litter mates were used. At the genomic level, m/m mice differ from wild-type mice only with respect to the introduced point mutations and a 52 bp insert (remaining *loxP* site and some flanking sequence) in the intron flanking the C1 domain exon (Figure 1A). Munc13-1-deletion mutant mice were described previously (Augustin et al., 1999b). Munc13-2 deletion mutant mice, which are essentially indistinguishable from wild-type controls, and Munc13-1/Munc13-2 double-deletion mutant mice will be described elsewhere (Rosenmund et al., 2002).

Cell Culture, Electrophysiology, and Semliki-Forest-Virus Infections

All electrophysiological experiments were performed on individual autaptic hippocampal neurons in microisland cultures (Bekkers and Stevens, 1991; Rosenmund et al., 1995). Data are expressed as mean $\pm$ SE. Significance was tested using Student's t test or one-way ANOVA with the Bonferroni-Dunn procedure for multiple comparisons (Instat). Semliki-Forest-Virus infections of neurons were performed as described (Ashery et al., 2000; Betz et al., 2001). Semliki-Forest-Virus constructs encoding Munc13-1-EGFP, ubMunc13-2-EGFP, and Munc13-1[H567K]-EGFP were published previously (Ashery et al., 2000; Betz et al., 2001). Hippocampal neurons were double labeled for Munc13-1 and Synaptophysin, as described previously (Augustin et al., 1999b).

Phosphorylation Experiments and Protein Analysis

Levels of PKCs were determined in brain homogenates of wild-type and Munc13-1[H567K]/Munc13-1[H567K] mice by SDS-PAGE and immunoblotting using commercially available antibodies (Transduction Laboratories). Immunolabeled bands were visualized by enhanced chemoluminescence (ECL; Amersham Pharmacia Biotech) and quantified densitometrically. For the analysis of β-PE-dependent phosphorylation of proteins in cultured neurons, cortical/hippocampal neurons from wild-type and m/m brains were plated at high density on polylysine/collagene. For radioactive labeling, cells were washed twice with phosphate-free MEM-Eagle medium and incubated in this medium for 2 hr in the presence of 0.2 mCi/ml [^{32}P] orthophosphate (Amersham Pharmacia Biotech). Cells were then stimulated with 1 μM PDBU for 1 hr, washed in phosphate-free MEM-Eagle medium, and harvested in extraction buffer (1% sodium cholate, 100 mM NaCl, 2 mM EGTA, 25 mM HEPES-KOH [pH 7.4], 5 μM microcystin LR, 20 mM NaF, 20 mM Na-pyrophosphate, 1 mM p-nitrophenyl phosphate, 1 μg/ml aprotinin, 0.5 μg/ml leupeptin, 0.2 mM phenylmethylsulfonyl fluoride) for 2D-electrophoresis or immunoprecipitation experiments. 2D electrophoresis (isoelectric focusing/SDS-PAGE) was performed using IPG-strips (pH 3–10; Amersham Pharmacia Biotech) in an IPGphor Isoelectric Focusing System (Amersham Pharmacia Biotech) for the first dimension and

the Mini Protean II System (Bio-Rad) for the second dimension. Gels were dried and analyzed by autoradiography. Immunoprecipitation of Munc13-1 was done as described with a specific polyclonal antibody (N395; Betz et al., 1997). Separated proteins were blotted to nitrocellulose and analyzed by immunoblotting with a monoclonal antibody to Munc13-1 (Betz et al., 1998) and ECL (Amersham Pharmacia Biotech). Immunoprecipitated Munc13-1 was quantified densitometrically. Phosphorylation of SNAP-25 and GAP-43 was analyzed by stimulating cortical/hippocampal neurons with 1 μM PDBU for 30 min. Cells were then washed with PBS and harvested for direct analysis by SDS-PAGE and immunoblotting using phosphopeptide-specific antibodies (Iwasaki et al., 2000; Kawakami et al., 2000).

References

Ashery, U., Varoqueaux, F., Voets, T., Betz, A., Thakur, P., Koch, H., Neher, E., Brose, N., and Rettig, J. (2000). Munc13-1 acts as a priming factor for large dense-core vesicles in bovine chromaffin cells. EMBO J. *19*, 3586–3596.

Augustin, I., Betz, A., Herrmann, C., Jo, T., and Brose, N. (1999a). Differential expression of two novel Munc13 proteins in rat brain. Biochem. J. *337*, 363–371.

Augustin, I., Rosenmund, C., Südhof, T.C., and Brose, N. (1999b). Munc13-1 is essential for fusion competence of glutamatergic synaptic vesicles. Nature *400*, 457–461.

Augustin, I., Korte, S., Rickmann, M., Kretzschmar, H.A., Südhof, T.C., Herms, J.W., and Brose, N. (2001). The cerebellum-specific Munc13 isoform Munc13-3 regulates cerebellar synaptic transmission and motor learning in mice. J. Neurosci. *21*, 10–17.

Bekkers, J.M., and Stevens, C.F. (1991). Excitatory and inhibitory autaptic currents in isolated hippocampal neurons maintained in culture. Proc. Natl. Acad. Sci. USA *88*, 7834–7838.

Betz, A., Okamoto, M., Benseler, F., and Brose, N. (1997). Direct interaction of the rat unc-13 homologue Munc13-1 with the N-terminus of syntaxin. J. Biol. Chem. *272*, 2520–2526.

Betz, A., Ashery, U., Rickmann, M., Augustin, I., Neher, E., Südhof, T.C., Rettig, J., and Brose, N. (1998). Munc13-1 is a presynaptic phorbol ester receptor that enhances neurotransmitter release. Neuron *21*, 123–136.

Betz, A., Thakur, P., Junge, H.J., Ashery, U., Rhee, J.-S., Scheuss, V., Rosenmund, C., Rettig, J., and Brose, N. (2001). Functional interaction of the active zone proteins Munc13-1 and RIM1 in synaptic vesicle priming. Neuron *30*, 183–196.

Brose, N., Hofmann, K., Hata, Y., and Südhof, T.C. (1995). Mammalian homologues of *C. elegans* unc-13 gene define novel family of C_2-domain proteins. J. Biol. Chem. *270*, 25273–25280.

Brose, N., Rosenmund, C., and Rettig, J. (2000). Regulation of transmitter release by Unc-13 and its homologues. Curr. Opin. Neurobiol. *10*, 303–311.

de Graan, P.N., Hens, J.J., and Gispen, W.H. (1994). Presynaptic PKC substrate B-50 (GAP-43) and neurotransmitter release: studies with permeated synaptosomes. Neurotoxicology *15*, 41–47.

Fabbri, M., Bannykh, S., and Balch, W.E. (1994). Export of protein from the endoplasmatic reticulum is regulated by a diacylglycerol/phorbol ester binding protein. J. Biol. Chem. *269*, 26848–26857.

Goda, Y., Stevens, C.F., and Tonegawa, S. (1996). Phorbol ester

effects at hippocampal synapses act independently of the gamma isoform of PKC. Learn. Mem. 3, 182–187.

Hawkins, R.D., Kandel, E.R., and Siegelbaum, S.A. (1993). Learning to modulate neurotransmitter release: themes and variations in synaptic plasticity. Annu. Rev. Neurosci. 16, 625–665.

Hessler, N.A., Shirke, A.M., and Malinow, R. (1993). The probability of transmitter release at a mammalian central synapse. Nature 366, 569–572.

Hoffman, D.A., and Johnston, D. (1998). Downregulation of transient K$^+$ channels in dendrites of hippocampal CA1 pyramidal neurons by activation of PKA and PKC. J. Neurosci. 18, 3521–3528.

Honda, I., Kamiya, H., and Yawo, H. (2000). Re-evaluation of phorbol ester-induced potentiation of transmitter release from mossy fibre terminals of the mouse hippocampus. J. Physiol. 529, 763–776.

Hori, T., Takai, Y., and Takahashi, T. (1999). Presynaptic mechanism for phorbol ester-induced synaptic poteniation. J. Neurosci. 19, 7262–7267.

Iwasaki, S., Kataoka, M., Sekiguchi, M., Shimazaki, Y., Sato, K., and Takahashi, M. (2000). Two distinct mechanisms underlie the stimulation of neurotransmitter release by phorbol esters in clonal rat pheochromocytoma PC12 cells. J. Biochem. 128, 407–414.

Kawakami, M., Iwasaki, S., Sato, K., and Takahashi, M. (2000). Erythropoietin inhibits calcium-induced neurotransmitter release from clonal neuronal cells. Biochem. Biophys. Res. Commun. 279, 293–297.

Kazanietz, M.G., Caloca, M.J., Eroles, P., Fujii, T., Garcia-Bermejo, M.L., Reilly, M., and Wang, H. (2000). Pharmacology of the receptors for the phorbol ester tumor promoters: multiple receptors with different biochemical properties. Biochem. Pharmacol. 60, 1417–1424.

Lackner, M.R., Nurrish, S.J., and Kaplan, J.M. (1999). Facilitation of synaptic transmission by EGL-30 G$_q\alpha$ and EGL-8 PLCβ: DAG binding to UNC-13 is required to stimulate acetylcholine release. Neuron 24, 335–346.

Lakso, M., Pichel, J.G., Gorman, J.R., Sauer, B., Okamoto, Y., Lee, E., Alt, F.W., and Westphal, H. (1996). Efficient in vivo manipulation of mouse genomic sequences at the zygote stage. Proc. Natl. Acad. Sci. USA 93, 5860–5865.

Majewski, H., and Iannazzo, L. (1998). Protein kinase C: a physiological mediator of enhanced transmitter output. Prog. Neurobiol. 55, 463–475.

Malenka, R.C., and Nicoll, R.A. (1999). Long-term potentiation—a decade of progress? Science 285, 1870–1874.

Miller, K.G., Emerson, M.D., and Rand, J.B. (1999). G$_o\alpha$ and diacylglycerol kinase negatively regulate the G$_q\alpha$ pathway in C. elegans. Neuron 24, 323–333.

Minami, N., Berglund, K., Sakaba, T., Kohmoto, H., and Tachibana, M. (1998). Potentiation of transmitter release by protein kinase C in goldfish retinal bipolar cells. J. Physiol. 512, 219–225.

Nayak, A., and Browning, M.D. (1999). Presynaptic and postsynaptic mechanisms of long-term potentiation. Adv. Neurol. 79, 645–658.

Nurrish, S.J., Segalat, L., and Kaplan, J.M. (1999). Serotonin inhibition of synaptic transmission: GOA-1 decreases the abundance of UNC-13 at release sites. Neuron 24, 231–242.

Oleskevich, S., and Walmsley, B. (2000). Phosphorylation regulates spontaneous and evoked transmitter release at a giant terminal in the rat auditory brainstem. J. Physiol. 526, 349–357.

Oleskevich, S., Clements, J., and Walmsley, B. (2000). Release probability modulates short-term plasticity at a rat giant terminal. J. Physiol. 524, 513–523.

Parfitt, K.D., and Madison, D.V. (1993). Phorbol esters enhance synaptic transmission by a presynaptic, calcium-dependent mechanism in rat hippocampus. J. Physiol. 471, 245–268.

Redman, R.S., Searl, T.J., Hirsh, J.K., and Silinsky, E.M. (1997). Opposing effects of phorbol esters on transmitter release and calcium currents at frog motor nerve endings. J. Physiol. 501, 41–48.

Richmond, J.E., Weimer, R.M., and Jorgensen, E.M. (2001). An open form of syntaxin bypasses the requirement for unc-13 in vesicle priming. Nature 412, 338–341.

Rosenmund, C., and Stevens, C.F. (1996). Definition of the readily releasable pool of vesicles at hippocampal synapses. Neuron 16, 1197–1207.

Rosenmund, C., Clements, J.D., and Westbrook, G.L. (1993). Non-uniform probability of glutamate release at a hippocampal synapse. Science 262, 754–757.

Rosenmund, C., Feltz, A., and Westbrook, G.L. (1995). Synaptic NMDA receptor channels have a low open probability. J. Neurosci. 15, 2788–2795.

Rosenmund, C., Sigler, A., Augustin, I., Reim, K., Brose, N., and Rhee, J.-S. (2002). Differential control of vesicle priming and short-term plasticity by Munc13 isoforms. Neuron, in press.

Sakaba, T., and Neher, E. (2001a). Quantitative relationship between transmitter release and calcium current at the calyx of Held synapse. J. Neurosci. 21, 462–476.

Sakaba, T., and Neher, E. (2001b). Preferential potentiation of fast-releasing synaptic vesicles by cAMP at the calyx of Held. Proc. Natl. Acad. Sci. USA 98, 331–336.

Shimazaki, Y., Nishiki, T., Omori, A., Sekiguchi, M., Kamata, Y., Kozaki, S., and Takahashi, M. (1996). Phosphorylation of 25-kDa synaptosome-associated protein. Possible involvement in protein kinase C-mediated regulation of neurotransmitter release. J. Biol. Chem. 271, 14548–14553.

Song, Y., Ailenberg, M., and Silverman, M. (1998). Cloning of a novel gene in the human kidney homologous to rat munc13s: its potential role in diabetic nephropathy. Kidney Int. 53, 1689–1695.

Stevens, C.F., and Tsujimoto, T. (1995). Estimates for the pool size of releasable quanta at a single central synapse and for the time required to refill the pool. Proc. Natl. Acad. Sci. USA 92, 846–849.

Stevens, C.F., and Sullivan, J.M. (1998). Regulation of the readily releasable vesicle pool by protein kinase C. Neuron 21, 885–893.

Voets, T. (2001). Dissection of three Ca^{2+}-dependent steps leading to secretion in chromaffin cells from mouse adrenal slices. Neuron 28, 537–545.

Waters, J., and Smith, S.J. (2000). Phorbol esters potentiate evoked and spontaneous release by different presynaptic mechanisms. J. Neurosci. 20, 7863–7870.

Yawo, H. (1999a). Protein kinase C potentiates transmitter release from the chick ciliary presynaptic terminal by increasing the exocytotic fusion probability. J. Physiol. 515, 169–180.

Yawo, H. (1999b). Two components of transmitter release from the chick ciliary presynaptic terminal and their regulation by protein kinase C. J. Physiol. 516, 461–470.